The Impact of Additive Manufacturing on the Acoustic Performance of Novel Porous Materials

Agnieszka Ciochon* and John Kennedy†
Trinity College Dublin, Dublin, D02 PN40, Ireland

Raphael Leiba‡
Trinity College Dublin, Dublin, D02 PN40, Ireland

Lara Flanagan§
Trinity College Dublin, Dublin, D02 PN40, Ireland

Commonly used conventional acoustic porous materials suffer from a limited operational frequency range and great dependency of the sample thickness on their performance. For this reason, acoustic metamaterials have caught the eye of the scientific community with their ability to manipulate and absorb soundwaves despite their subwavelength dimensions. These novel acoustic materials are especially of interest for aerospace and automotive industries. Industrially relevant design tools are required to unlock the potential of these materials and the development of these tools requires benchmark problems. This work analyzes how the additive manufacturing process influences the acoustic performance of a periodic porous acoustic material. To answer this question, samples of a benchmark material were fabricated using selective laser melting with a 0.03 mm layer height. An optical microscope, a confocal microscope and computerized tomography scanner were used to examine manufactured specimens and provide insight into their surface topology. Numerical models of the structure were created. The computational results were compared with the experimental values. A combination of modelling strategies are investigated to incorporate features of the additive manufacture in the prediction of the acoustic behaviour. The observed mismatch between them can only partially be explained by the presence of the surface roughness. This study emphasizes the need to take into account more aspects of the additive manufacturing process when designing acoustic materials.

I. Introduction

The limitations of conventional acoustic treatments created the need to develop more advanced noise solutions. For many years, acoustic metamaterials have captivated much scientific interest as they are characterized by superior absorptive behaviour targeting specified frequency ranges. Metamaterials are usually designed as arrays of subwavelength unit cells and rely on their geometries to create local resonances across the whole structure [1]. For that reason, their performance often arises from the geometrical design, rather than from material properties of composites, from which they were manufactured.

Although the first acoustic metamaterials have been proposed over 20 years ago, to this day they remain mostly as a scientific curiosity and have not progressed towards being commercialized at an industrial scale. The working principles behind some of the designs neither take into account the real-world operating conditions, nor the performance realistic of industrial applications. The major issues hindering the practical development of acoustic metamaterials include their small scale features, mechanical properties and large-scale fabricability [2].

The creation of such complex and small scale structures required advances in the production technology. Additive manufacturing (AM) opened the possibility to fabricate complex geometries, with internal features that could not

*PhD Candidate, Department of Mechanical, Manufacturing & Biomedical Engineering, Trinity College Dublin, the University of Dublin, College Green, D02 PN40, Ireland, aciochon@tcd.ie

†Assistant Professor, Department of Mechanical, Manufacturing & Biomedical Engineering, Trinity College Dublin, the University of Dublin, College Green, D02 PN40, Ireland, jkenned5@tcd.ie

‡Research Fellow, Department of Mechanical, Manufacturing & Biomedical Engineering, Trinity College Dublin, the University of Dublin, College Green, D02 PN40, Ireland, leibar@tcd.ie

§PhD Candidate, Department of Mechanical, Manufacturing & Biomedical Engineering, Trinity College Dublin, the University of Dublin, College Green, D02 PN40, Ireland, flanagl1@tcd.ie

otherwise be fabricated using traditional subtractive methods [3]. The advancements of AM could soon develop into a mass production technique, however, the impact of the manufacturing strategy on the acoustic behaviour of designs must first be understood. Various AM technologies exist on the market, differing in running costs and process complexity. The dimensional accuracy and surface quality of produced parts increase with the sophistication of the chosen AM technique, however, no manufacturing strategy is free from imperfections. Therefore, the additively manufactured parts often require additional post-processing.

Excessively rough surface finish of additively manufactured parts arises as a result of the layer-by-layer fabrication, which is the working principle of all AM technologies. The quality of components manufactured in such a manner is therefore generally lower than of parts produced with the usage of traditional techniques, such as numerical control machines [4]. One of the major factors contributing to the formation of rough surface finish is the tessellation of the CAD geometry. During the process, original surfaces are approximated, which can lead to a deformation of the initial shape during slicing. Tessellated computer-aided design (CAD) data files often contain flaws such as overlaps, gaps or degenerate facets and may require correction in an additional repair software [5]. This is a significant issue since many new acoustic materials require accurate manufacture of features at the sub-millimetre scale [6, 7].

The staircase effect is another manufacturing error that originates from the deposition of sliced layers. Layer height is therefore a factor contributing significantly to the final roughness of printed surfaces. The surface quality of components produced via extrusion-based AM technologies is generally worse than of liquid resin type processes, like stereolithography (SLA) [8] or powder based processes such as selective laser melting (SLM) [9]. SLM is one of the most advanced technologies that utilise metal powders and are able to achieve the highest accuracy and superior mechanical properties of printed parts. However, the formation of surface roughness and its effect remains similar across all of the AM technologies.

Despite its many advantages, SLM is also subject to the stair step effect, which occurs during approximation of curvatures. Although the layer height is significantly smaller in comparison to other AM technologies, components manufactured using SLM are still subject to surface quality issues. This remains a key limitation since the post-processing of metal parts is costly and time consuming [10]. Roughness in SLM is also affected by the balling effect, during which the melt pool gets broken into spherical particles that settle on created surfaces. Not only does this phenomenon constrict creation of sharp geometries, but also leads to irregular deposition of material onto the former layer, which can lead to porosity and delamination between layers [11].

Another challenge associated with the topic presents itself in an adequate choice and definition of a parameter to be used for description of the roughness effect arising from the additive manufacturing of acoustic materials. The surface roughness average Ra, which according to the BS EN 10049:2013 is defined as a mean deviation of the distance between the measurement centreline and the surface profile, is an industry standard used for surface evaluation. However, it should be treated as just a broad insight into the measured surface as it is an average and may be too general to describe non-isotropic surfaces having sharp peaks and deep valleys [12]. The main issue is that totally different surface topologies may give the same average roughness value. Therefore, in order to accurately be able to draw a link between the acoustic performance and the roughness effect, a new surface parameter may be required.

There is little research reporting the effects of AM process on the acoustic performance of metamaterials. This is of importance as layer-by-layer fabrication leads to geometric distortion and produced structures vary from ideal CAD assumptions. Most studies have compared experimental data with numerical or analytical results, assuming homogeneous surfaces and not taking manufacturing into account. Researchers have not treated the issue of arising surface roughness in much detail and used it to explain the gap between these results without further investigations [13–15].

Therefore, the goal of this research is to analyse the formation of surface roughness and understand its influence on the acoustic performance of additively manufactured materials. This work takes the form of a case-study of the benchmark porous material that was fabricated with a SLM-based 3D Systems Prox DMP 200 machine using a standard layer height of 0.03 mm. Corresponding cross-sectional sample of the structure was manufactured for a comprehensive investigation of the surface topology. Numerical models of the structure were composed. Moreover, manufactured samples were also experimentally tested for sound absorption in an impedance tube.

II. Benchmark Material

The porous material, which was the subject of this study, was developed as a part of the European COST action DENORMS (Designs for Noise Reducing Materials and Structures) [16]. The structure is a lattice of periodically arranged unit cells. The DENORMS cell is a cube with a spherical internal cavity, which is connected to adjacent cells by cylindrical openings on each of its faces.

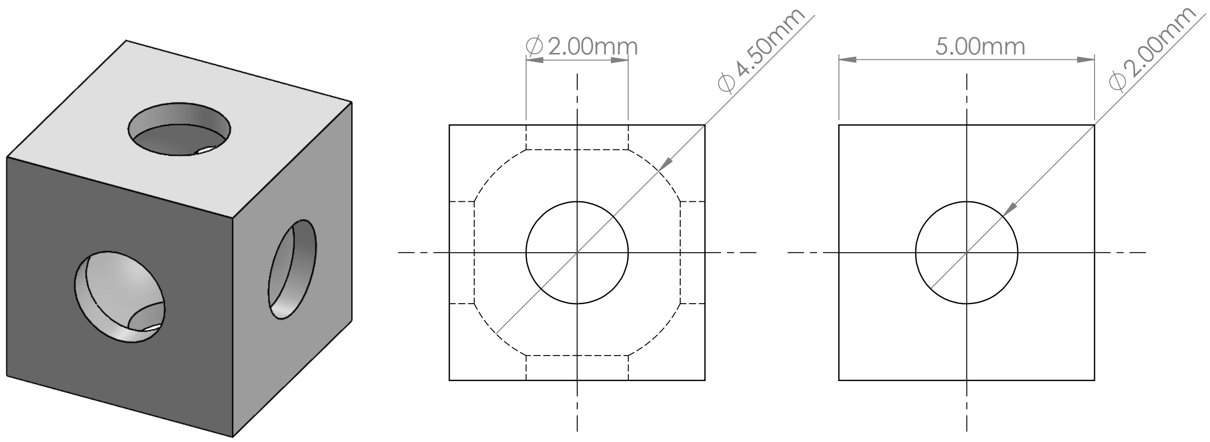

Fig. 1 DENORMS unit cell geometry

The main advantage of this relatively simple design is that it is easy to produce and to post-process. Moreover, the geometry depends on just a few parameters that can be easily tuned to achieve desired acoustic behaviour. In this paper, the DENORMS cell had an internal spherical cavity of a 2.25 mm radius connected to six cylindrical cavities having a 1 mm radius. The cavity was embedded into a cube with a 5 mm wall length, as shown in Figure 1.

In theory, every cell should be isotropic and act as a chain of resonators inside the structure for incident sound waves. In reality, however, the fabrication process is responsible for creation of the roughness effect and has influence on the acoustic behaviour of the whole system.

In this work, three cylindrical samples suitable for impedance tube measurements and one cross-sectional sample suitable for surface topology investigation were fabricated with a SLM-based 3D Systems Prox DMP 200 using steel powder, as shown in Figure 2.

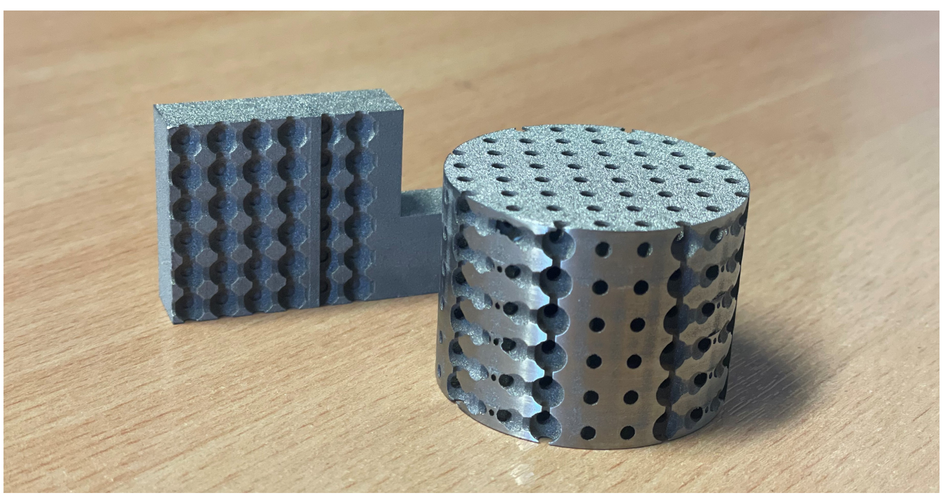

Fig. 2 Samples manufactured for confocal microscope (cross-sectional) and sound absorption (cylidrical) testing

III. Industrially Relevant Inspection Procedures

Several non-destructive testing (NDT) techniques were implemented into this study as inspection methods for the quality control of fabricated parts. They provide an in-depth insight into the surface topology and are a useful tool for evaluation of component properties. Furthermore, NDT enables defect detection without the need to destroy the part, which is especially crucial in AM.

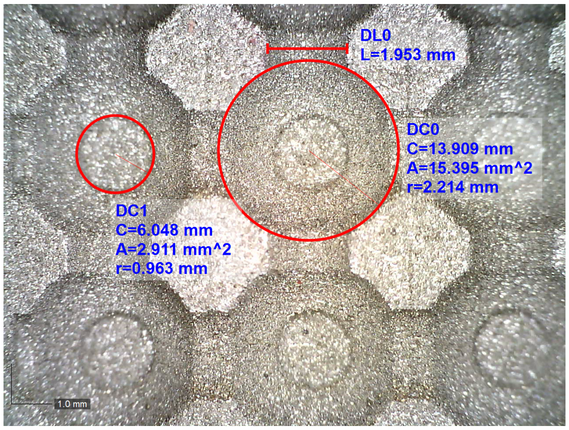

(a) Cross-sectional sample

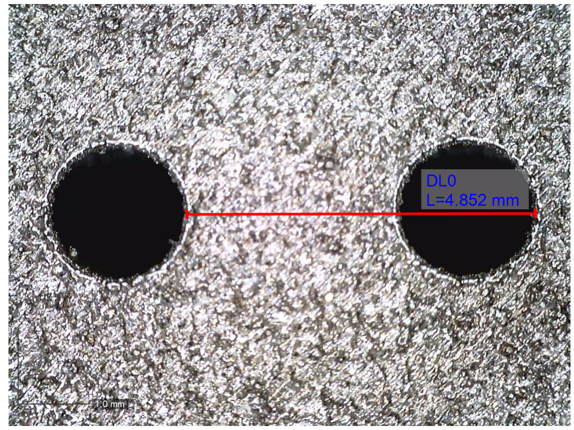

(b) Top of a cylindrical sample

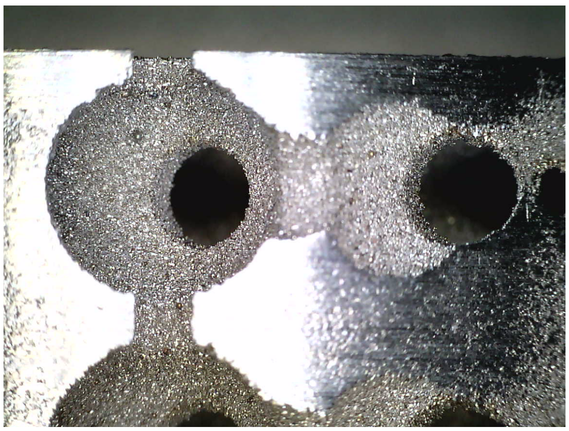

(c) Surface finish of cavities

(d) Satelite particle

Fig. 3 Microscopic images of DENORMS samples

A. Digital Microscopy

The Dino-Lite Premier AM7013MT digital microscope was used to capture close up pictures of surface of both samples. It has a 5 Megapixels sensor and is able to magnify up to 200x magnification with a resolution of up to 2592x1944.

Microscopic pictures of cylindrical and cross-sectional samples are illustrated in Figure 3. Figure 3a shows a close up of the cross-sectional sample and displays the geometrical accuracy of the printer in capturing the set CAD drawing. As can be seen, the geometrical fidelity has been better achieved by the printer during creation of cylinders rather than spheres. This distortion of the internal geometries will lead to a small change in the frequency of the peak absorption performance.

Figure 3b displays the top of the cylindrical sample. As can be seen, the distance between adjacent cells falls below the set 5 mm, which can be caused by distortion of cylinder heights. The roughness of the inner cavities is shown in Figure 3c. It should be noted that the cylindrical samples underwent sanding on the outside face in order to fit better into the sample holder of the impedance tube. A satellite particle can be spotted on the surface of the cavity in the upper left corner, which appeared as a result of the balling effect. Figure 3d shows it in more detail. These additional, relatively large scale, features on the surface will also disrupt the visco-thermal boundary layer development and potentially lead to enhanced losses in the material.

B. Confocal Microscopy

An automated, 3-axis measuring instrument developed internally in Trinity College Dublin was used to examine additively manufactured components, as shown Figure 4. The machine acquires 2D line scans of the inspected surface by moving an automated XY stage, on top of which the part is fixed, across the path of a Keyence CL-PT010 chromatic confocal sensor (spot diameter of ø 3.5 μm, linearity of ±0.22 μm and resolution of 0.25 μm). This system is used for surface roughness measurements and evaluation of dimensional accuracy.

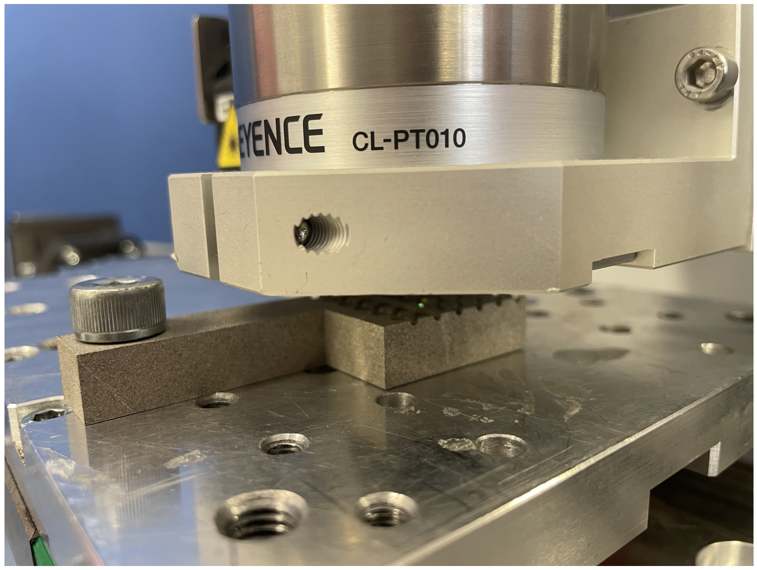

Fig. 4 Confocal microscope

A representative surface profile acquired for the manufactured cross-sectional sample is illustrated in Figure 5. The obtained profile is a combination of three separate measurements with a measurement centreline set at three different heights so that the whole cell is captured. The periodicity of the rough surface profile can be related to the manufacturing layer height but there are additional irregular roughness features. These are likely due to the complexity of the processes occurring within the melt pool during manufacture. The formation of satellite particles is a random process and their distribution across the surface is possibly linked with the local curvature of the surface within the cell. The periodic nature of the layer height lends itself to simple implementation into the numerical models of the surface but the additional random features present a greater challenge.

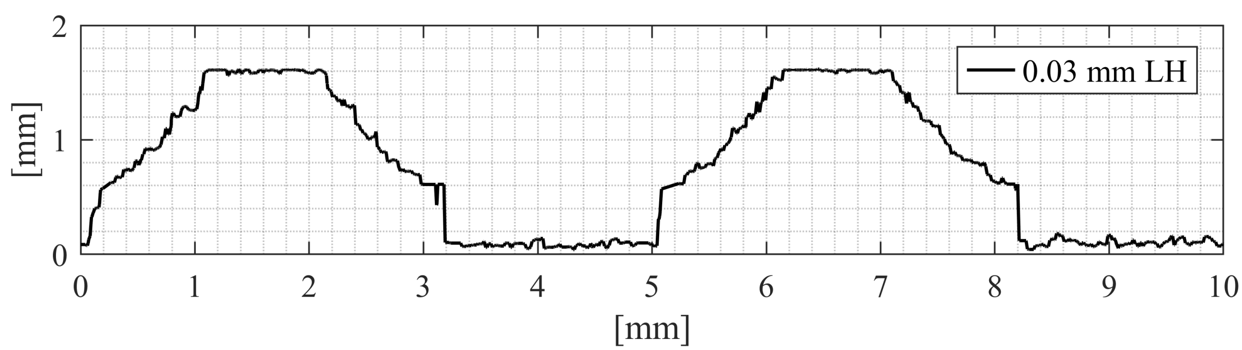

Fig. 5 Surface profile

C. CT Scanning

The XT H 225 ST industrial computed tomography (CT) system available at Trinity College Dublin was used to inspect internal components of the fabricated part. The SLM sample was imaged at 225kV, 93 μmA with a 2 s exposure time, 18dB gain using a 2.5mm Al filter and W (Tungsten) target. The effective pixel size was 8 μm. A subsection of the cylindrical sample was extracted by EDM cutting for inspection within the CT machine. The subsection was taken from the centre of the cylindrical sample and was sufficiently small for the CT scan to penetrate inside the structure.

The analyzed sample is shown in the upper left corner of the Figure 6. Figure 6 displays a horizontal slice across the structure at the middle height of the DENORMS cell. The scan reveals that the sample's walls are relatively porous. Moreover, there are discontinuities present at edges of the surfaces which connect the bulk air volume with porous cavities within the metal walls. There is evidence of connected cavities which are branching deeper inside the solid structure.

The impact of this surface porosity on the acoustic behaviour is unclear. These features are irregular and randomly distributed across the unit cell. The size of the open volumes and the nature of their connection to the main air cavity can be established from the CT scan data but a strategy to model these features and their impact on the target acoustic behaviour is not a trivial issue.

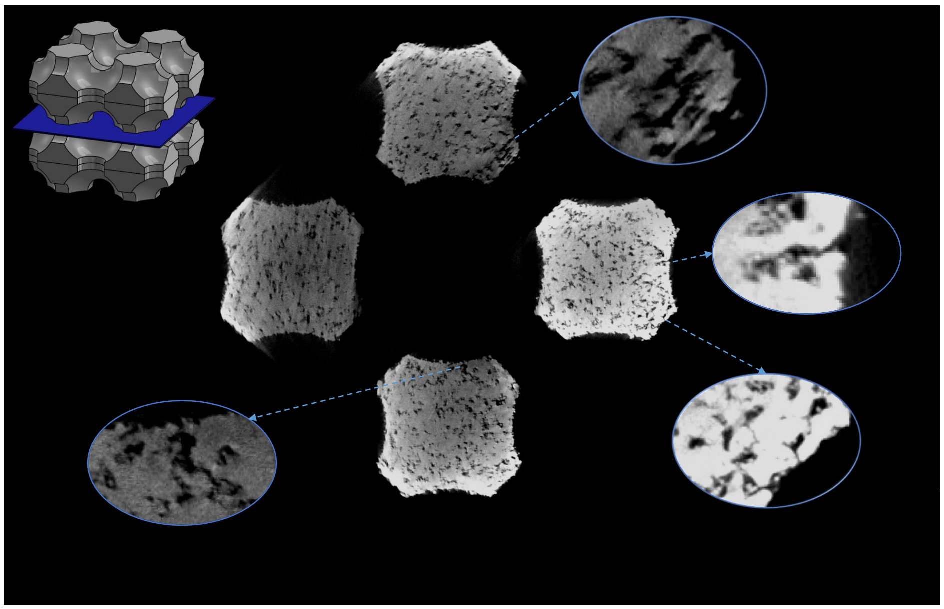

Fig. 6 Horizontal slice of a cut SLM part obtained with CT scan

IV. Acoustic Assessment

A. Experimental Testing

The sound absorption tests of manufactured samples were performed according to ISO 10534-2 using an impedance tube in a normal incidence setup, where the sample face is exposed to plane waves. The testing procedure has been previously implemented in [6, 15–18]. The custom rig, shown in Figure 7, with a 40mm internal diameter was used for these tests with an upper frequency limit of 5000Hz. The lower limit is determined by the speaker and is in the region of 300 Hz. On the right hand side of Figure 7 we can see the BMS 4591 speaker which is driven by the output signal of a National Instruments DAQ which has been amplified by a power amplifier. GRAS 40PL array microphones were chosen to instrument the rig as they have a frequency response (± 1 dB) in the region of 50 Hz - 5 kHz and upper limit of the dynamic range of 135 dB re 20 μPa allowing for testing up to high pressure amplitudes. The microphones are connected to the National Instruments DAQ and the signals were recorded using a MATLAB interface. The microphones were calibrated using the switching methods described in ISO 10534-2. Each of three samples was measured three times, with the full disassembly and reassembly of the sample holder, so the repeatability of the test procedure would be taken into consideration.

B. Numerical Modelling Strategy

The numerical modelling was conducted in a commercial finite element analysis software COMSOL Multiphysics. The DENORMS structure was solved using the Thermoviscous Acoustics interface that is suitable for modelling microacoustics. It enables proper inclusion of thermal and viscous losses occurring within the boundary layer. The

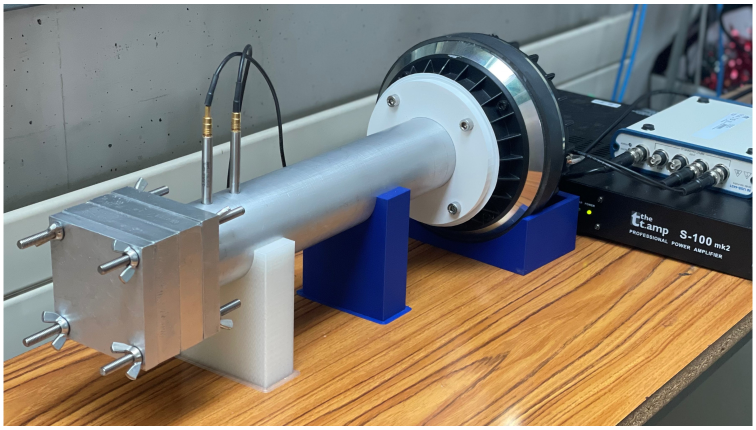

Fig. 7 Impedance tube

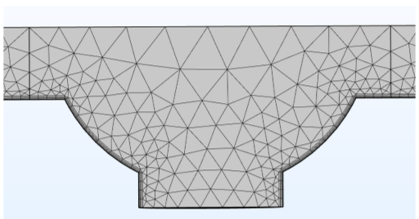

(a) Smooth mesh

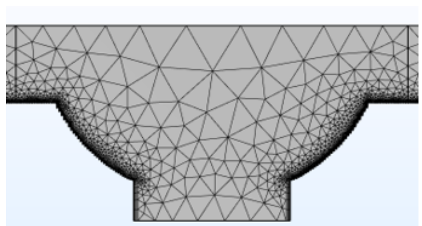

(b) Rough mesh

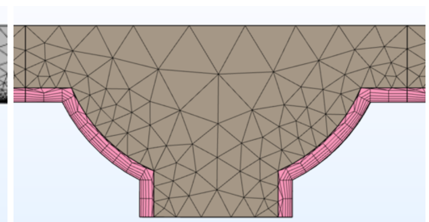

(c) Fluid shell mesh

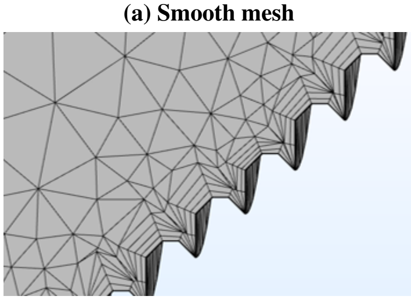

(d) Rough geometry close-up

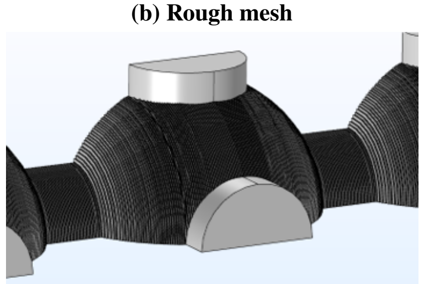

(e) Rough geometry

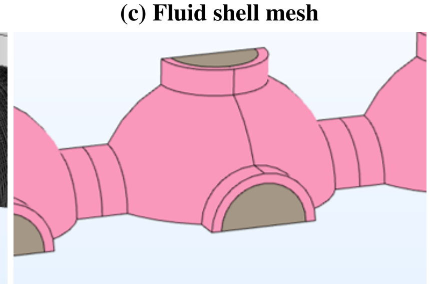

(f) Fluid shell geometry

Fig. 8 Numerical models

modelling strategy was previously implemented in [15, 17]. The generated models correspond to a structure with six layers of the unit cell. Due to the isotropic character of the DENORMS geometry, only a quarter of cells was modelled in order to reduce the computational time. Furthermore, symmetrical conditions were applied to the side channels, which ensured a correct approach towards modelling infinite material in two dimensions.

Generated geometries are illustrated in Figure 8. Fig 8a shows mesh of the original geometry with a hard, smooth wall finish. However, due to the layer-by-layer manufacturing, the assumption of the perfectly smooth surfaces of the DENORMS cell is false. Therfore, a rough pattern, which corresponded to the 0.03 mm layer height, was applied to all main surfaces. The mesh of the created geometry is depicted in Figure 8b. Figure 8d shows the boundary layer mesh along the roughness grooves in more detail. A unit cell of the rough geometry in 3D is displayed in Figure 8e.

Although meshing and modelling of rough geometry is possible, it requires high computational resources. To reduce the computational cost of the modelling, a new approach was implemented into the third geometry. The unit cell was divided into two sections: the inner region being air, and an outer fluid shell (FS) with altered air properties. In the fluid shell, all air properties were kept the same except the dynamic viscosity μ, which was altered in a parametric sweep. The rough surface will lead to an increase in boundary layer thickness and to increased losses compared to the smooth geometry. This fluid shell layer is intended to modify the growth of the boundary layer through the altered dynamic viscosity. The extend of the fluid shell was chosen as five times the boundary layer thickness of the smooth model.

The mesh of the fluid shell geometry is shown in Figure 8c. A unit cell of this geometry in 3D is depicted in Figure 8f. The air is depicted in brown colour, and outer fluid shell with increased dynamic viscosity is shown in pink.

V. Results and Discussion

The results of all elements of the study are shown in Figure 9. An initial comparison should be drawn between the experimental result and the smooth numerical curve. The approximate peak locations are 1925 Hz for the experimental and 2050 Hz for the numerical, the magnitude of the peak is also significantly underestimated. When we consider the rough surface model there is a shift of the numerical peak to a lower frequency, closer to the experimental value. There is also a small increase in the peak magnitude. The fluid shell modelling approach has greater success in predicting the magnitude of the experimental curve. The lower frequency peak location is also captured in this modelling approach. This suggests that the fluid shell modelling approach may be useful as a relatively low cost addition to the modelling approach which can capture some of the features of the manufacturing. The next steps will require the formalisation of the extent of the fluid shell region and a modification of the dynamic viscosity based a target boundary layer development.

It should be noted however that there is clear evidence of a higher broadband absorption in the experimental values due to the different curve shape. It is unlikely that the modelling strategies utilised here will capture this effect even when optimised for the correct prediction of the peak location and amplitude. These additional broadband losses will require explanation through investigation of the fundamental physics which may call into question some of the assumptions in the visco-thermal modelling.

The modelling strategies here attempt to directly resolve the physical processes that drive the losses within the structure. Alternative approaches include equivalent fluid modelling of the whole structure but the calibration of the model constants is a difficult problem in these approaches. It is hoped that the work presented here will lead to clear guidelines on the impact of surface roughness on the acoustic behaviour of additively manufactured materials. This knowledge could then be fed into a variety of modelling strategies to account for these effects.

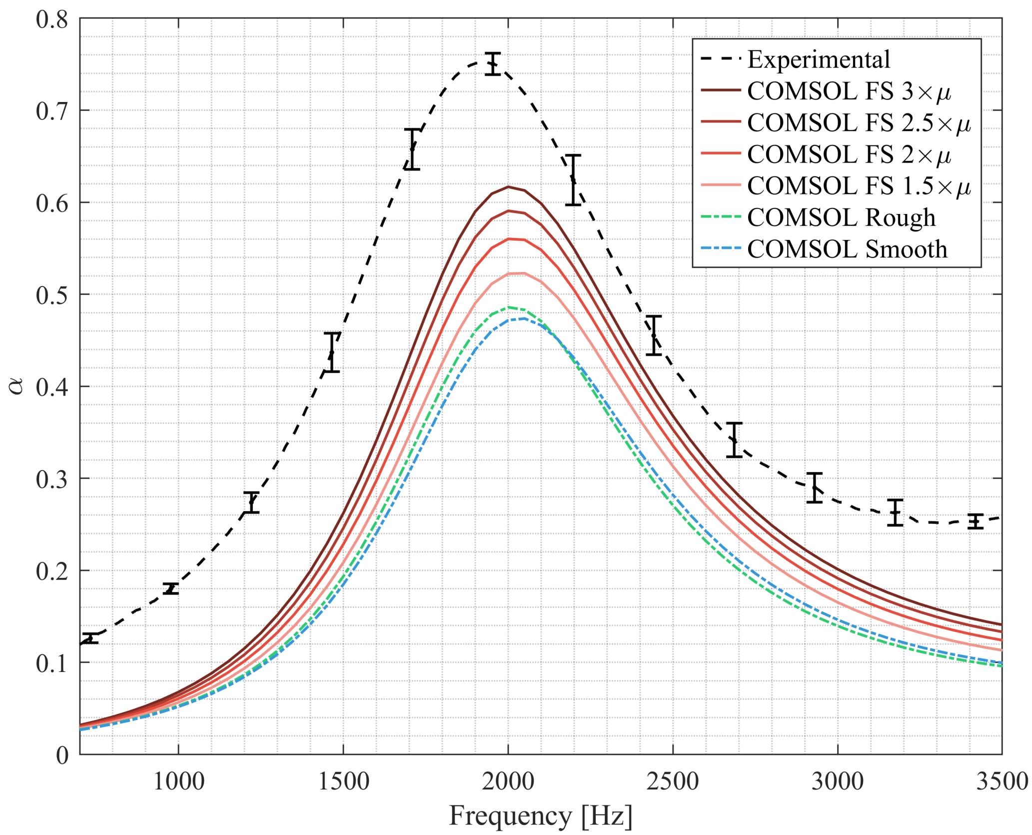

Fig. 9 Experimental and numerical results

Acknowledgments

This work was funded through IRC Postgraduate Award GOIPG/2019/2927 "Advanced acoustic metamaterials for noise reduction, optimised for additive manufacturing technologies".

The authors wish to acknowledge the COST Action DENORMS (CA 15125) and in particular Dr. Tomasz G. Zielinski, Department of Intelligent Technologies, Institute of Fundamental Technological Research of the Polish Academy of Sciences who proposed the design of the unit DENORMS cell.

The authors wish to acknowledge the AMBER Additive Research Lab in the facilitating of the manufacturing of our metal test specimens and the AR Lab staff on providing training and guidance on the manufacturing process. The AR-Lab has been enabled by a 3.3M award from Science Foundation Ireland as part of their Research Infrastructure program and an additional 1M investment from the European Research Council.

References

[1] Ma, G., and Sheng, P., "Acoustic metamaterials: From local resonances to broad horizons," *Science Advances*, Vol. 2, No. 2, 2016, p. e1501595. https://doi.org/10.1126/sciadv.1501595.

[2] Cummer, S. A., Christensen, J., and Alù, A., "Controlling sound with acoustic metamaterials," *Nature Reviews Materials*, Vol. 1, No. 3, 2016, p. 16001. https://doi.org/10.1038/natrevmats.2016.1.

[3] Townsend, A., Senin, N., Blunt, L., Leach, R. K., and Taylor, J. S., "Surface texture metrology for metal additive manufacturing: a review," *Precision Engineering*, Vol. 46, 2016, pp. 34–47. https://doi.org/10.1016/j.precisioneng.2016.06.001.

[4] Rahmati, S., and Vahabli, E., "Evaluation of analytical modeling for improvement of surface roughness of FDM test part using measurement results," *The International Journal of Advanced Manufacturing Technology*, Vol. 79, No. 5-8, 2015, pp. 823–829. https://doi.org/10.1007/s00170-015-6879-7.

[5] Mohan Pandey, P., Venkata Reddy, N., and Dhande, S. G., "Slicing procedures in layered manufacturing: a review," *Rapid Prototyping Journal*, Vol. 9, No. 5, 2003, pp. 274–288. https://doi.org/10.1108/13552540310502185.

[6] Rice, H., Kennedy, J., Göransson, P., Dowling, L., and Trimble, D., "Design of a Kelvin cell acoustic metamaterial," *Journal of Sound and Vibration*, Vol. 472, 2020, p. 115167. https://doi.org/10.1016/j.jsv.2019.115167.

[7] Mao, H., Rumpler, R., Gaborit, M., Göransson, P., Kennedy, J., O'Connor, D., Trimble, D., and Rice, H., "Twist, tilt and stretch: From isometric Kelvin cells to anisotropic cellular materials," *Materials & Design*, Vol. 193, 2020, p. 108855. https://doi.org/10.1016/j.matdes.2020.108855.

[8] Kim, M. K., Lee, I. H., and Kim, H.-C., "Effect of fabrication parameters on surface roughness of FDM parts," *International Journal of Precision Engineering and Manufacturing*, Vol. 19, No. 1, 2018, pp. 137–142. https://doi.org/10.1007/s12541-018-0016-0.

[9] Dowling, L., Kennedy, J., O'Shaughnessy, S., and Trimble, D., "A review of critical repeatability and reproducibility issues in powder bed fusion," *Materials & Design*, Vol. 186, 2020, p. 108346. https://doi.org/10.1016/j.matdes.2019.108346.

[10] Strano, G., Hao, L., Everson, R. M., and Evans, K. E., "Surface roughness analysis, modelling and prediction in selective laser melting," *Journal of Materials Processing Technology*, Vol. 213, No. 4, 2013, pp. 589–597. https://doi.org/10.1016/j.jmatprotec.2012.11.011.

[11] Mumtaz, K., and Hopkinson, N., "Top surface and side roughness of Inconel 625 parts processed using selective laser melting," *Rapid Prototyping Journal*, Vol. 15, No. 2, 2009, pp. 96–103. https://doi.org/10.1108/13552540910943397.

[12] Sahay, C., and Ghosh, S., "Understanding Surface Quality: Beyond Average Roughness (Ra)," *2018 ASEE Annual Conference & Exposition Proceedings*, ASEE Conferences, 2018, p. 31176. https://doi.org/10.18260/1-2--31176.

[13] Xu, Z.-x., Meng, H.-y., Chen, A., Yang, J., Liang, B., and Cheng, J.-c., "Tunable low-frequency and broadband acoustic metamaterial absorber," *Journal of Applied Physics*, Vol. 129, No. 9, 2021, p. 094502. https://doi.org/10.1063/5.0038940.

[14] Kone, T. C., Lopez, M., Ghinet, S., Dupont, T., and Panneton, R., "Thermoviscous-acoustic metamaterials to damp acoustic modes in complex shape geometries at low frequencies," *The Journal of the Acoustical Society of America*, Vol. 150, No. 3, 2021, pp. 2272–2281. https://doi.org/10.1121/10.0006441.

[15] Kennedy, J., Flanagan, L., Dowling, L., Bennett, G. J., Rice, H., and Trimble, D., "The Influence of Additive Manufacturing Processes on the Performance of a Periodic Acoustic Metamaterial," *International Journal of Polymer Science*, Vol. 2019, 2019, pp. 1–11. https://doi.org/10.1155/2019/7029143.

[16] Zieliński, T. G., Opiela, K. C., Pawłowski, P., Dauchez, N., Boutin, T., Kennedy, J., Trimble, D., Rice, H., Van Damme, B., Hannema, G., et al., "Reproducibility of sound-absorbing periodic porous materials using additive manufacturing technologies: Round robin study," *Additive Manufacturing*, Vol. 36, 2020, p. 101564.

[17] Flanagan, L., Heaphy, D., Kennedy, J., Leiba, R., and Rice, H., "Development of acoustic "meta-liners" providing sub-wavelength absorption," *International Journal of Aeroacoustics*, Vol. 19, No. 6-8, 2020, pp. 310–323.

[18] Deery, D., Flanagan, L., O'Brien, G., Rice, H. J., and Kennedy, J., "Efficient Modelling of Acoustic Metamaterials for the Performance Enhancement of an Automotive Silencer," *Acoustics*, Vol. 4, No. 2, 2022, pp. 329–344.